



Full length article

Synergistic regenerative effects of functionalized endometrial stromal cells with hyaluronic acid hydrogel in a murine model of uterine damage



Yoon Young Kim^{a,1}, Kyu-Hyung Park^{a,1}, Yong Jin Kim^b, Moon Suk Kim^c, Hung Ching Liu^d, Zev Rosenwaks^d, Seung-Yup Ku^{a,*}

^a Department of Obstetrics and Gynecology, Seoul National University Hospital, Seoul, South Korea

^b Department of Obstetrics and Gynecology, Korea University Guro Hospital, Seoul, South Korea

^c Department of Molecular Technology, Ajou University, Suwon, South Korea

^d Center for Reproductive Medicine and Infertility, Weill Cornell Medical College, New York, NY, USA

ARTICLE INFO

Article history:

Received 4 November 2018

Received in revised form 6 March 2019

Accepted 14 March 2019

Available online 18 March 2019

Keywords:

Endometrial regeneration

Hydrogel

Hyaluronic acid

Endometrial stromal cells

Decidualization

ABSTRACT

Clinically intractable infertility and recurrent miscarriage due to irreversible endometrial damage need to be treated with biomaterial- and cell-based therapies. Some previous studies have reported on the efficacy of a collagen scaffold and/or bone marrow-derived mesenchymal stem cells. However, the functional differentiation of grafted cells was uncertain, and the time required for regeneration was long in these studies.

Here, we show the synergistic regenerative effects of hyaluronic acid (HA) hydrogel with *in vitro* decidualized endometrial stromal cells (EMSCs) in a murine uterine infertility (synechiae) model. Decidualized EMSCs (dEMSCs) were encapsulated with HA hydrogel, combined with three different doses of fibrinogen/thrombin (5, 50, and 500 mIU/mL). The HA/fibrin gel showed biocompatibility when mixed with dEMSCs. The addition of thrombin enhanced gel formation (5 and 50 mIU/mL) and engraftment and enabled the effective release of adhesion molecules.

Within two weeks, which is a short duration, treatment with hydrogel decreased the fibrous tissue and increased the thickness of the endometrium. The regenerated endometrium demonstrated functional recovery, as evidenced by the expression and secretion of molecules essential for embryonic implantation, such as Desmin, CD44, PECAM, and IGF-1. Transferred embryos successfully implanted and the normal development of implanted embryos ($n = 37$) were evaluated by co-localization of distinct markers of the three germ layers (Sox2, Nestin, Brachyury, AFP, and HNF4 α). Live birth of offspring was achieved in the regenerated endometrium by HA hydrogel.

Therefore, HA hydrogel-mixed dEMSCs can be an innovative treatment strategy with rapid recovery of endometrial damage and may also have therapeutic potential in intractable infertility or recurrent miscarriage.

Statement of Significance

Decidualized EMSCs (dEMSCs) encapsulated with HA hydrogel combined with fibrinogen/thrombin (50 mIU/mL) showed injectability and biocompatibility when mixed with dEMSCs.

Hydrogel-encapsulated dEMSCs can be a useful treatment for damaged endometrium in short duration, with successful implantation and normal development in a murine model.

© 2019 Acta Materialia Inc. Published by Elsevier Ltd. All rights reserved.

* Corresponding author at: Department of Obstetrics and Gynecology, Seoul National University College of Medicine, 101 Daehak-Ro, Jongno-Gu, Seoul 03080, South Korea.

E-mail address: jyhsyk@snu.ac.kr (S.-Y. Ku).

¹ These authors contributed equally to this work.

1. Introduction

Irreversible endometrial damage possibly causes infertility or uterine symptoms such as Asherman's syndrome [1–3]. Of particular importance are uterine factors involved in infertility or recurrent miscarriage, as recovery from these conditions is difficult owing to irreversible endometrial damage [4]. Therefore, new

therapeutic strategies such as cell- and/or biomaterial-based treatments are required.

The endometrium provides an optimal milieu that is critical for embryo implantation through the secretion of cytokines and growth factors [5]. This specialized tissue regularly undergoes morphological and functional changes, following a temporal cycle under the control of sex hormones such as estrogen (E_2) and progesterone (P_4) [6,7]. To maintain these specialized cycles, the endometrium possesses highly proliferative somatic cells: the endometrial stromal cells (EMSCs).

EMSCs differentiate into decidual cells during early secretory and early pregnancy phases [8]. Optimized decidualization is critical for successful embryonic implantation and trophoblastic growth in most mammals including humans, nonhuman primates, and rodents [9]. When decidualization does not occur correctly, embryos cannot attach for implantation, and they do not develop further in *in vivo*. During decidualization, the expression of specific genes such as those for prolactin (PRL) [10] and insulin-like growth factor (IGF) [11] is induced. In addition, EMSCs undergo morphological changes from a spindle to a polygonal shape. To be utilized for the treatment of irreversible endometrial damage, donor EMSCs can be decidualized *in vitro* through a combined treatment with the ovarian steroid hormones P_4 and E_2 [12]. The endometrium expresses cluster of differentiation (CD) molecules, which act as either receptors or ligands in the endometrium. In the uterus, CD44 is involved in the adhesion process during embryonic implantation and is locally expressed on the endometrial epithelium [13]. Owing to its limited expression during the implantation period, CD44 is thought to play a role in the initial trophoblast–endometrial interaction [14].

The nonsulfated glycosaminoglycan hyaluronic acid (HA) is a linear polysaccharide composed of repeating β -1,4-D-glucuronic acid- β -1,3-N-acetyl-D-glucosamine disaccharide units, and its derivatives have recently been recognized as efficacious biomaterials that can be used in many fields of tissue engineering and regenerative medicine [15].

In the uterus, HA plays a role during trophoblast invasion into the maternal endometrium [16]. It has been used as a replacement for albumin in embryo cultures *in vitro* [17]. Therefore, we considered HA to could be an appropriate molecule for endometrial regeneration therapeutics owing to the existence of HA receptor in the endometrium. Fibrin is a biomatrix that is formed when fibrinogen (F) is mixed with thrombin (T). It is plausible that composite hydrogels made from a combination of fibrin and HA may be able to support successful embryonic implantation, considering their compatibility with the intrauterine environment.

Previous studies have mainly used bone marrow-derived mesenchymal stem cells (BM-MSCs) [18,19] or EMSCs [20] as cell sources for uterine regeneration therapies. However, collagen sheets combined with rat BM-MSCs required three months for endometrial regeneration [21]. Similarly, BM-MSCs showed regenerative ability in mice but required three estrus cycles for regeneration [22]. In rats, human embryonic stem cell-derived endometrium-like cells also showed regenerative potential during a functional recovery period of three months [23]. Although some studies have reported the efficacy of BM-MSCs [22] and/or collagen scaffolds [21] in rodent endometrial injury models, the time required for regeneration is long and the degree of functional differentiation of the grafted cells is uncertain. To date, little is known about whether *in vitro* processed endometrial cells encapsulated in composite matrix scaffolds are effective as a therapeutic option when administered into the cavity of damaged endometria.

In this study, we aimed to construct endometrium-tailored HA/fibrin composite hydrogels and investigate their regenerative effects in combination with *in vitro* decidualized EMSCs (dEMSCs) in a murine uterine synechia model.

2. Materials and methods

2.1. Ethics

Eight-week-old male and female C57BL/6 mice were maintained in the animal facility of Seoul National University Hospital. Five mice were housed per cage in a room with a 12-hour light/dark cycle and unlimited access to food and water. All of the animal experimental procedures were approved by the Seoul National University Hospital Institutional Animal Care and Use Committee [IACUC, No.16-0005-S1A0(4)].

2.2. Preparation of endometrial stromal cells and *in vitro* decidualization

2.2.1. Isolation of donor endometrial stromal cells (EMSCs)

Uterine horns of 8-week-old female mice were incised longitudinally to expose the uterine cavity and were cut into small pieces. After washing with HBSS (Invitrogen, Waltham, MA, USA), uterine tissues were incubated with HBSS containing 1 mg/mL collagenase type I (Invitrogen) and 50 IU/mL penicillin-streptomycin (P/S, Invitrogen) for 1 h at 37 °C. Tissues were minced and then passed through a 70- μ m cell strainer (BD Biosciences, San Jose, CA, USA). Cells were re-suspended in Dulbecco's modified Eagle's medium/F12 (DMEM/F12, Invitrogen), containing 10% fetal bovine serum (FBS, HyClone, Logan, Utah, USA) and 50 IU/mL P/S. After an initial culture of 30 min, the medium was changed to remove residual epithelial cells and further cultured in fresh medium.

2.2.2. *In vitro* decidualization of EMSCs

EMSCs were seeded at a density of 1×10^5 cells/well and cultured until they reached 80% density. Decidualization was induced by adding 0.1 nM E_2 (Sigma-Aldrich, St. Louis, MO, USA) and 100 nM of P_4 (Sigma-Aldrich) in phenol red-free DMEM/F12 (Invitrogen) supplemented with 10% FBS and 50 IU/mL P/S and culturing cells for an additional 10 days. The spindle-shaped EMSCs transformed into large rounded cells, which resembled *in vivo* decidua. Culture supernatants were collected and stored at -20 °C until they were assayed for prolactin (PRL) concentration.

2.2.3. Flow cytometry analysis

Cells were detached using 0.25% trypsin-EDTA (Invitrogen) and sequentially blocked, centrifuged, rinsed, and resuspended in PBS at a concentration of 10^5 cells/mL. Resuspended cells were incubated with 5 μ L of fluorescein isothiocyanate-labeled anti-mouse-CD44, -CD49f, and -CD73 antibodies (BD Pharmingen, San Jose, CA, USA) in the dark at 24 °C for 30 min. After washing twice with PBS, cells were analyzed using a flow cytometer (BD FACS Calibur™, BD Biosciences).

2.2.4. Measurement of prolactin (PRL) concentration

Culture supernatants were collected and stored at -20 °C until assayed. The concentration of PRL in collected supernatants was measured using an immunoassay kit (Abcam, Cambridge, UK) according to the manufacturer's protocol. Briefly, supernatants were added to a 96-well plate and incubated with antibody mixture. After incubation, the wells were washed to remove unbound material, and 3,3',5,5'-tetramethylbenzidine (TMB) substrate was added. The reaction was then stopped, and absorbance was measured at 450 nm using a UniCel DxI Access system (Beckman Coulter, Indianapolis, IN, USA).

2.3. Preparation of injectable hydrogel composite

2.3.1. Preparation of injectable HA/fibrin hydrogel

Select-HA™ 150 K (mol. wt 125–175 kDa) was purchased from Sigma-Aldrich, and gelation was performed according to the manufacturer's protocol. The HA powder was solubilized to 1% (w/v) concentration in the supplied solvent. The HA solution was then placed in a flask and cooled to 5 °C in a water bath with stirring. F and each concentration of T (5, 50, and 500 mIU/mL) [24] were separately prepared in a single syringe and were connected to a joining piece. Then, F and HA were then mixed with T to prepare an injectable HA/fibrin hydrogel.

2.3.2. Rheological measurement of HA/fibrin hydrogel

Viscosity was assessed using a cone-and-plate digital viscometer (LVT Wells-Brookfield, Brookfield Engineering Laboratories, Stoughton, MA, USA). All measurements were performed at 37 °C in 0.5 mL of test fluid. The experimental conditions for the detection of gel formation were as follows: temperature 37 °C, shear strain 0.05%, shear stress 1 Pa, and oscillation frequency 1 Hz. The electronic system detected and stored the storage modulus (G' in Pa) and the loss modulus (G'' in Pa) at a frequency of 1 Hz. The pressure of the upper plate on the gel was set to 1 Pa and automatically controlled during the gelation process.

2.3.3. Encapsulation of dEMSCs using HA/fibrin hydrogel

In vitro decidualized EMSCs (dEMSCs) were harvested using 0.25% trypsin-EDTA (Invitrogen), washed twice with PBS (Invitrogen), and centrifuged. Washed cells were mixed with HA by gentle pipetting, and F and each concentration of T (5, 50, 500 mIU/mL) were added sequentially, immediately before intrauterine injection.

2.3.4. Scanning electron microscopy (SEM) analysis

Samples were fixed with 2.5% glutaraldehyde (Sigma-Aldrich) and subsequently fixed with 2% aqueous osmium tetroxide (Sigma-Aldrich) and serially dehydrated. Samples were then chemically dried using hexamethyldisilazane (HMDS). Images were captured using a scanning electron microscope (SEM; S-3700N, Hitachi, Tokyo, Japan).

2.3.5. Cell proliferation assay

The viability of dEMSCs was determined using a tetrazolium salt, 2-(4-iodophenyl)-3-(4-nitrophenyl)-5-(2,4-disulfophenyl)-2 H tetrazolium, monosodium salt (WST-1) assay kit (Roche Diagnostics, Indianapolis, IN, USA). Briefly, cells were seeded at a density of 1×10^4 cells/well on 96-well plates and incubated in a 5% CO₂ atmosphere at 37 °C for 48 h. The medium was removed, and samples were washed three times with PBS. The WST-1 reagent was then reconstituted to 10% with media and was added to the plate, which was incubated for 2 h at 37 °C in the dark. The absorbance of the supernatant from each well was measured at 480 nm with a UV-visible spectrophotometer (VersaMax, Molecular Devices, Sunnyvale, CA, USA). Each experiment was performed in triplicate.

2.4. Establishment of murine model with endometrial damage

Eight-week-old C57BL/6 female mice were used to induce endometrial damage. A mixture of 8 μ L of Zoletil (Virbac, Hamilton, New Zealand) and 2 μ L of Rompun (Bayer, Leverkusen, Germany) was used for anesthesia. After administration of Zoletil/Rompun by intraperitoneal injection, 50% ethanol was infused through the uterine cervix using a 24-gauge IV catheter (BD Biosciences), and the endometrial cavity was irrigated with saline 5 min later. After one week, a vertical incision was made on the abdominal wall, and

uteri were collected. The degree of damage was evaluated depending on morphological observation of hematoxylin and eosin (H&E)-stained tissue sections.

2.5. Regeneration of endometrium using HA/fibrin hydrogel with dEMSCs

2.5.1. *In utero* tracking using CM-Dil

Decidualized EMSCs were prelabeled with CM-Dil (C7000, Invitrogen) for postinjection tracking *in utero*. Uterine horns containing CM-Dil-labeled dEMSCs encapsulated with hydrogels were excised at day 14, embedded in OCT (Scigen, Gardena, CA, USA), and frozen at –30 °C for 10 min. Finally, the frozen tissues were serially sectioned at a thickness of 6 μ m using a cryostat (Leica), and fluorescence images were captured using an EVOS-FL fluorescence microscope.

2.5.2. Injection of HA/fibrin hydrogel with dEMSCs into uterine cavity

Mice were assigned to each of four treatment groups, namely, HA, HA + F + T5, HA + F + T50, and HA + F + T500 (Table 3). Hydrogels with dEMSCs were injected 7 days after the induction of uterine damage. Cells (1×10^7), in combination with hydrogel scaffolds, were injected as a bolus of 100 μ L through the uterine horn after a small dorsal incision was made.

2.5.3. Embryo transfer and evaluation of embryonic implantation

Functional recovery of engrafted uteri was evaluated by the occurrence of pregnancy after embryo transfer (ET). Donor embryos to be transferred were retrieved from pregnant uteri (E3.0) by saline irrigation through the syringes. Under isoflurane anesthesia, five embryos in 20 μ L of M2 medium (Sigma-Aldrich) were loaded onto a capillary tube (BD Biosciences) and transferred to each uterine horn of untreated or engrafted recipient mice. On posttransfer days 5 and 8, uteri were removed and stained with 10% Evans blue solution (Sigma-Aldrich), and the number of implanted sites was counted. Implantation efficiency was calculated as the ratio of the number of implanted embryos to the total number transferred (Table 4).

2.6. Histological analyses

All samples used for histological analyses were surgically collected, fixed with 10% formalin for more than 12 h, dehydrated in ethanol, and embedded in paraffin. Horizontal sections were prepared at 5- μ m intervals and stained by either H&E or Masson Trichrome staining method as given in previous reports [25].

2.7. Immunofluorescence analysis

To assess cell compatibility, cells were fixed with 4% paraformaldehyde (PFA) for 15 min at room temperature and then rinsed with PBS. Samples were labeled with the primary antibody rabbit antimouse desmin (1:100, Santa Cruz Biotechnology, Dallas, Texas, USA) at 4 °C overnight. Samples were then rinsed three times in PBST for ~15 min each. The secondary antibody Alexa Fluor™ 488-conjugated donkey antirabbit (Molecular Probes, Waltham, MA, USA), was added, and the samples were incubated for 1 h at room temperature. Samples were then rinsed three times with PBST and incubated briefly with 10 μ g/mL 4',6-diamidino-2-phenylindole, dihydrochloride (DAPI, Sigma-Aldrich). Fluorescence images were captured using an EVOS-FL fluorescence microscope (Thermo Fisher Scientific, Waltham, MA, USA).

For immunohistochemistry analysis, tissue sections were labeled with the following primary antibodies, rabbit antimouse-CD44 (1:100, Santa Cruz Biotechnology), rabbit antimouse-Ki67 (1:100, Santa Cruz Biotechnology), goat antimouse platelet

endothelial cell adhesion molecule (PECAM) (1:200, Santa Cruz Biotechnology), and rabbit antimouse insulin-like growth factor (IGF)-1 (1:200, Santa Cruz Biotechnology). Samples were treated with the secondary antibodies antirabbit horse radish peroxidase (HRP, DAKO, Glostrup, Denmark) or anti-goat HRP (1:100, DAKO) for 2 h at room temperature and then washed three times with TBST (TBS with 0.05% Tween 20). The substrate, DAB, was then added, and slides were incubated at room temperature for 5 min. Finally, 10 µg/mL DAPI was added, and images were observed under a microscope (Leica, Nussloch, Germany).

2.8. Quantitative real-time reverse transcription PCR (qRT-PCR)

Specific primers used for qRT-PCR are listed in Table 1. Total RNA was isolated using TRIzol[®] reagent (Invitrogen). Complementary DNA was synthesized from 1 µg of purified total RNA using AccuPower RT PreMix (Bioneer, Daejeon, Korea), according to the manufacturer's instruction. PCR analysis was performed in a Rotor-Gene Q instrument (Qiagen, Valencia, CA, USA) using a QuantiTect SYBR green PCR kit (Qiagen) at the uniplex setting. The amplification program included an initial denaturation at 95 °C for 10 min, followed by 30 cycles of denaturation at 95 °C for 15 s, annealing at 58 °C for 20 s, and extension at 72 °C for 30 s. All reactions were performed in triplicate, and relative gene expression was normalized to GAPDH expression (see Table 2).

2.9. Immunostaining of implanted embryos

Embryo-implanted uterus samples were fixed with 10% formalin for 12 h and then rinsed with PBS. Samples were sequentially processed with water, 70% ethanol (EtOH), 80% EtOH, 90% EtOH, and 100% EtOH for 30 min each at room temperature. Samples were then processed in xylene (Sigma-Aldrich) for 30 min at room temperature, soaked with melted Paraplast (Sigma-Aldrich), and solidified as a paraffin block for sectioning. Solidified paraffin blocks were cut at a thickness of 5 µm using a microtome (Leica) and then transferred to microscope slides. Slides were dried overnight and stored at room temperature until ready for use.

To prepare samples for immunostaining, slides were placed in an oven at 56 °C for 10 min to melt the paraffin, and slides were then deparaffinized in xylene for 5 min. The slides were then incubated in 100% alcohol thrice for 3 min each and transferred to 95% EtOH for 3 min. Finally, slides were rinsed with PBS twice for 5 min each. After rinsing with PBS, samples were permeabilized in PBST

Table 1
Gelation time of HA/fibrin hydrogels with different thrombin concentrations.

Hydrogel group (n = 5)	HA + F + T5	HA + F + T50	HA + F + T500
HA	1%	1%	1%
T	5 mIU/mL	50 mIU/mL	500 mIU/mL
Gelation time (S)	22 ± 5	12 ± 5	5 ± 3

HA: hyaluronic acid, F: fibrinogen, T: thrombin.

Table 2
Primers used for qRT-PCR.

Abbreviation	Gene	Sequences	
		Forward	Reverse
GAPDH	Glyceraldehyde-3-phosphate dehydrogenase	5'-GTGTTCTACCCCAATGTG-3'	5'-ATAGGGCCTCTTCTGCTCAG-3'
Cdh1	Cadherin-1	5'-TGAAGATAGAGGCCGCAAT-3'	5'-CCAAGAACATGGGAGGCTCAT-3'
Esr	Estrogen receptor	5'-CAGTAACAAGGGCATGGAAC-3'	5'-GTACATGTCCCACCTTCTGAC-3'
FN	Fibronectin	5'-CGAGGTGACAGAGACCACAA-3'	5'-CTGGAGTCAAGCCAGACACA-3'
IGF-1	Insulin-like growth factor 1	5'-ACCGAGGGGCTTTACTTCA-3'	5'-TGGCTCACCTTCTTCTTCC-3'
LIF	Leukemia inhibitory factor	5'-AACTGGCAGCTCAATGG-3'	5'-AGGCGCACATAGCTTTTCC-3'
VEGF	Vascular endothelial growth factor	5'-GCACAAGGACGGCTTGAAGAT-3'	5'-CCCACGACAGAAGAGCAGA-3'

for 30 min at room temperature and blocked in blocking buffer, which consisted of PBS containing 3% bovine serum albumin (BSA, Sigma-Aldrich) and 0.3% Triton X-100 (Sigma-Aldrich). The primary antibodies mouse antimouse Sox2 (Abcam), rabbit antimouse Brachyury (Abcam), mouse antimouse Nestin (Abcam), goat antimouse AFP (Santa Cruz Biotechnology), mouse antimouse Brachyury (Santa Cruz Biotechnology), and rabbit antimouse HNF4α (Santa Cruz Biotechnology) were diluted 1:100 in blocking buffer. Samples were incubated with primary antibodies overnight at 4 °C. They were then rinsed three times in PBST for ~15 min each. The secondary antibodies Alexa Fluor[™] 488-conjugated donkey antirabbit, Alexa Fluor[™] 586 donkey antimouse, Alexa Fluor[™] 594-conjugated donkey antimouse, and Alexa Fluor[™] 594-conjugated donkey antirabbit (Molecular Probes, Waltham, MA, USA) were diluted 1:200 in blocking buffer. Samples were incubated in secondary antibodies for 1 h at room temperature, rinsed three times with PBST, and then incubated briefly with 10 µg/mL DAPI reagent. Fluorescence images were captured using a confocal microscope (Leica).

2.10. Statistical analysis

All values are presented as mean ± standard deviation (SD). Data were analyzed by ANOVA, followed by Bonferroni's test for multiple comparisons using the SPSS program (SPSS 12.0; SPSS, Inc., Chicago, IL, USA). A *P* value <0.05 was considered statistically significant.

3. Results

A schematic representation of the staged experimental procedures is shown in the graphical abstract, and the number of animals used in these experiments is given in Table 3.

3.1. Preparation of EMSCs and in vitro decidualization

For the analysis of properties of isolated endometrial stromal cells, we performed immuno-phenotyping of EMSCs from immature and parous mice. EMSCs isolated from uteri were found to

Table 3
Number of animals used.

	a	b	Total
EMSC donor	10		10
Embryo donor	54		54
Treated			
post-treatment analyses	2	32	42
post-implantation analyses	8		
Nontreated			
post-treatment analyses	2	8	12
post-implantation analyses	2		
Normal control	4		4
Total	82	40	122

EMSC: endometrial stromal cell, a: histology and PCR, b: implantation rate analysis.

express CD44, CD49f, and CD73. The CD44-positive population was the most prevalent population in parous EMSCs (64.7% vs. 50.7%), while populations positive for CD49f (87.3% vs. 53.5%) and CD73 (24.8% vs. 18.1%) were the most prevalent population in immature EMSCs (Fig. 1A). These experiments were performed in triplicate, and the pattern of expression was similar among replicate experiments.

The morphology of decidualized parous EMSCs changed to a polygonal shape, which is the typical morphology of decidual cells, whereas the immature EMSCs did not effectively undergo morphological changes (Fig. 1B). The concentration of prolactin, as a marker of decidualization, released into the culture medium was also higher in parous EMSCs than in immature EMSCs ($P < 0.01$, Fig. 1C).

3.2. Characterization of injectable HA/fibrin hydrogel with dEMSCs

3.2.1. Preparation of injectable HA/fibrin hydrogel with dEMSCs

An injectable hydrogel was constructed by combining 1% HA/F with various concentrations of T. The addition of F and T to HA facilitated the formation of networks, and gelation time was noted (Table 1). HA/fibrin injectable gels prepared with 50 and 500 IU/mL T showed networks with more biocompatible pores than HA + F + T5 gels and those containing HA-only (Fig. 2A). The stiffness of injectable HA/fibrin gels was measured by multiple rheometry. The addition of 50 mIU/mL T led to the formation of gels with higher stiffness than HA-only and HA + F + T5 gels. Thrombin at a 10-fold higher concentration (T500) also resulted in gel formation with the highest stiffness; however, these gels were less practical to use as scaffolds owing to their mechanical strength. Gel viscosities were in the range of 1.0×10^2 to 2.5×10^3 Pa·s, and viscosity generally increased with T concentration (Fig. 2B). The average Pa·s value of each group was 0.4, 3.16×10^2 , 1.37×10^3 , and 1.43×10^3 , respectively.

3.2.2. Characterization HA/fibrin hydrogel with dEMSCs

The biocompatibility of HA/fibrin-dEMSCs was evaluated by SEM. The cross-linked cells in the hydrogels maintained their morphology and were well integrated. SEM analysis revealed that collagen fibers were visible in the extracellular space. The formation of a connective network within HA/fibrin-dEMSCs was facilitated after incubation. After 4 h, small aggregated cell clusters were observed, and after 24 h, larger cell aggregates that were well integrated into the HA/fibrin scaffold were observed (Fig. 2C).

Distribution of dEMSCs within each hydrogel was evaluated, and the distribution pattern of HA/fibrin-dEMSCs within hydrogels varied depending on the concentration of thrombin, i.e., as the concentration of thrombin increased, the connectivity between cells significantly increased (Fig. 2D).

Hydrogel compatibility was confirmed by the expression of Desmin, a muscle fiber protein found in the uterus. The positively stained region showed a dense fiber structure. This fiber network was enhanced by the addition of 50 and 500 IU/mL T, whereas HA and HA + F + T5 gels formed a less dense fiber network (Fig. 2E). Such interconnected porous architecture in the HA/fibrin gel could provide a passageway for media, nutrients, and oxygen, which would support the survival and proliferation of the injected dEMSCs. When the viability of cells mixed with the hydrogels was assessed, active proliferation was observed; however, the proportion of proliferative cells, measured by WST-1 assays, was not significantly different among the hydrogels with different T concentrations (Fig. 2F).

The expression of cadherin-1 and fibronectin, which are the main adhesion and ECM molecules in the endometrium, was significantly upregulated in the HA + F + T gel group ($P < 0.01$, Fig. 2G). These results suggest that the addition of T to HA/fibrin hydrogels increases their adhesive properties by increasing the

expression of cell adhesion- and ECM-related genes. The maintenance of decidual characteristics in HA/fibrin hydrogels was evaluated by assessing the expression of decidual-specific genes. IGF-1 and ER expression was higher in HA/fibrin hydrogels than in those containing only HA ($P < 0.01$, Fig. 2H).

Holistically, these results indicated that the addition of 50 mIU/mL T resulted in the most effective environment for the construction of injectable cell-containing hydrogels that maintained the features of dEMSCs and showed enhanced biocompatibility.

3.3. Establishment of a murine model of endometrial damage

Induction of endometrial damage in mice was achieved by vaginal injection of ethanol. After 14 days, damage in the endometrium was evaluated by histological analysis. Damaged uteri demonstrated endometrial layers that were significantly thinner or indistinguishable from the myometrium. The thickness of the remaining endometrium was measured, and its average in the damaged model was in the range of 30–80 μm (Fig. 3A, left panel).

3.4. Endometrial regeneration in mouse models using HA/fibrin hydrogels with dEMSCs

3.4.1. Histological evaluation of endometrial regeneration after engraftment

Two weeks following the engraftment of the HA/fibrin hydrogels with dEMSCs, the engrafted uteri showed regeneration of the endometrial layer, displaying the presence of well-distributed cells and more apparent neovascularization (Fig. 3A). Furthermore, the stromal part of the tissue showed a well-organized structure, with epithelia and secretory glands. The thickness of the endometrial layers in the uteri treated with HA/fibrin hydrogels was significantly higher than that of the group treated with HA only ($P < 0.01$), with the HA + F + T50 hydrogel group showing the most effective endometrial regeneration (Fig. 3A right panel).

For the analysis of fibrous tissue, collagen content was evaluated. The image clearly showed that the HA + F + T50 hydrogel group with higher fibrous tissue (blue) contents demonstrated a larger amount of viable tissue (red) and a smaller amount of fibrous tissue (blue) than the nontreated group and HA-only or HA + F + T50 groups (Fig. 3B).

3.4.2. Analyses of endometrial regeneration after engraftment of HA/fibrin hydrogels

The proliferation of dEMSCs after engraftment was confirmed by assessing the expression of Ki67 in uteri isolated 14 days after engraftment. A higher proportion of Ki67-positive cells were observed in engrafted animals. Cells double-positive for Ki67 and CM-DiI were considered engrafted cells. The migration of engrafted cells was traced using the live cell dye CM-DiI. Positively stained regions were distributed in the uterine cavity, and the signal was increased in the HA + F + T50 group. In addition, CM-DiI-positive regions co-localized with Desmin-positive cells (Fig. 3C). Taken together, these data indicated that the injected cells were successfully engrafted in the damaged endometrium.

The expression of CD44, the main HA receptor that regulates cell–cell interactions, was also significantly increased in the HA/fibrin groups. The expression of PECAM and IGF-1, which are neovascularization- and decidual-specific genes, also significantly increased in the hydrogel-engrafted groups compared with those in the HA-only group. The majority of the PECAM signal localized near the generated glands and was also higher in hydrogel-engrafted groups ($P < 0.01$, Fig. 3D).

To analyze the effects of hydrogel on endometrial regeneration, VEGF and LIF expression was assessed. Significantly higher expression of these genes was observed in HA/fibrin hydrogel-treated

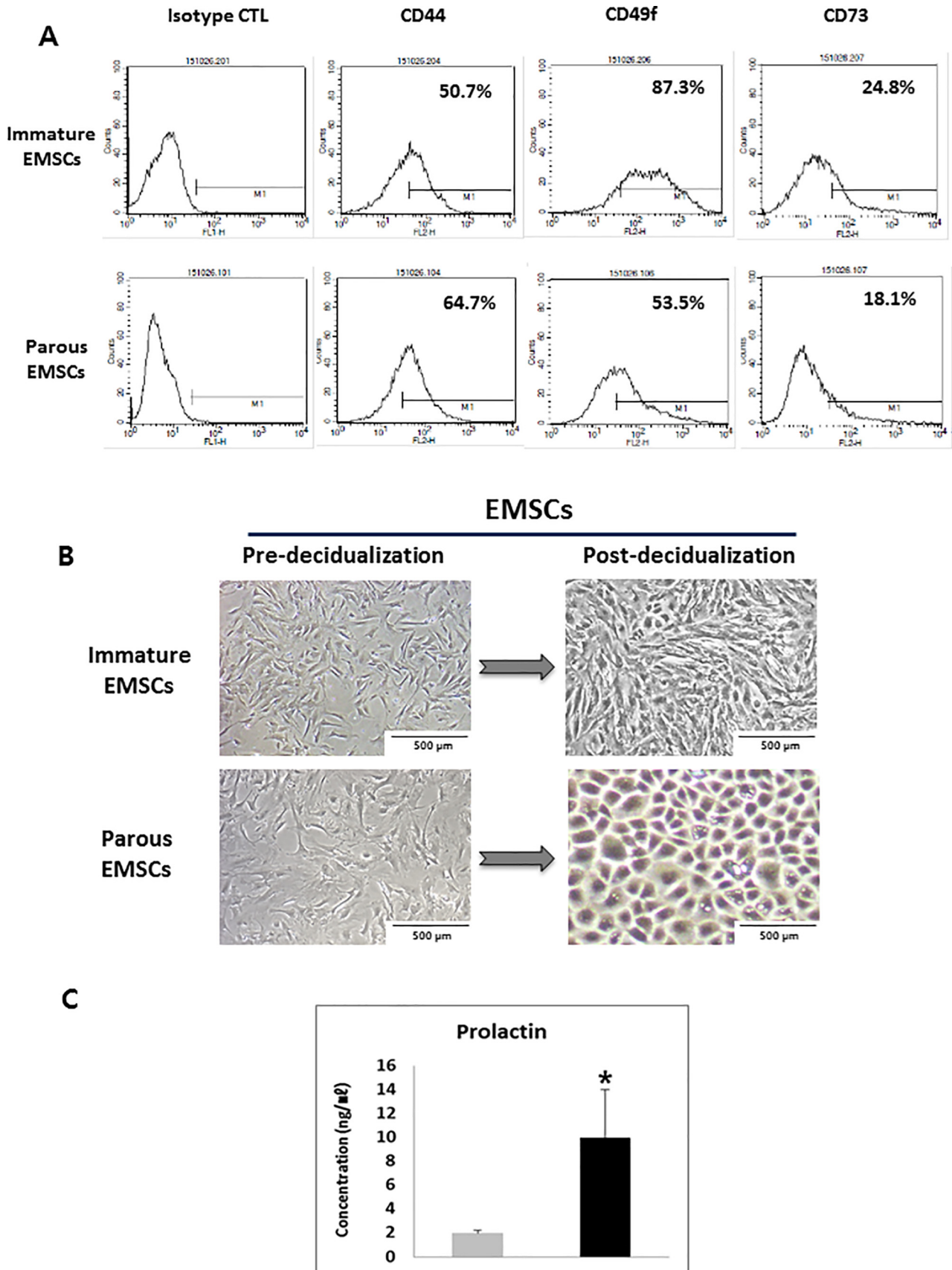


Fig. 1. Immuno-phenotyping and *in vitro* decidualization of EMSCs. Initial characterization of EMSCs was performed using a single cell-antibody reaction, and the transition to decidua was induced. The degree of decidualization was evaluated by measuring the secretion of prolactin (PRL). A. Immune phenotypes of isolated EMSCs were analyzed by FACS. The experiments of CD expression were conducted in triplicate batches, and the results were found similar among the experiments. B. EMSCs from immature and parous mice were treated with estrogen and progesterone, and decidualization was effectively achieved in the parous group. C. Decidualization was confirmed by measuring the secretion of prolactin into the medium. CTL: control, EMSCs: endometrial stromal cells.

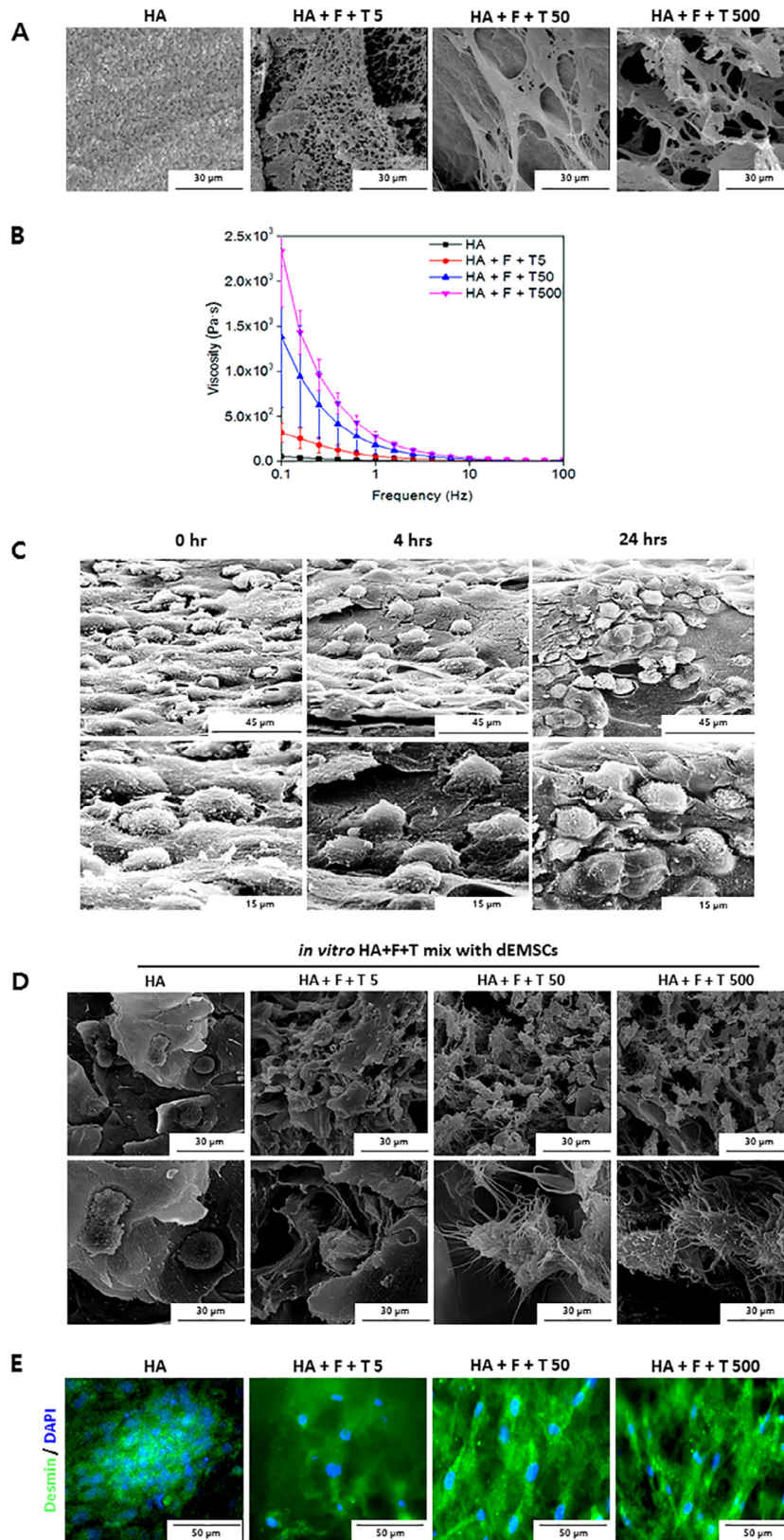
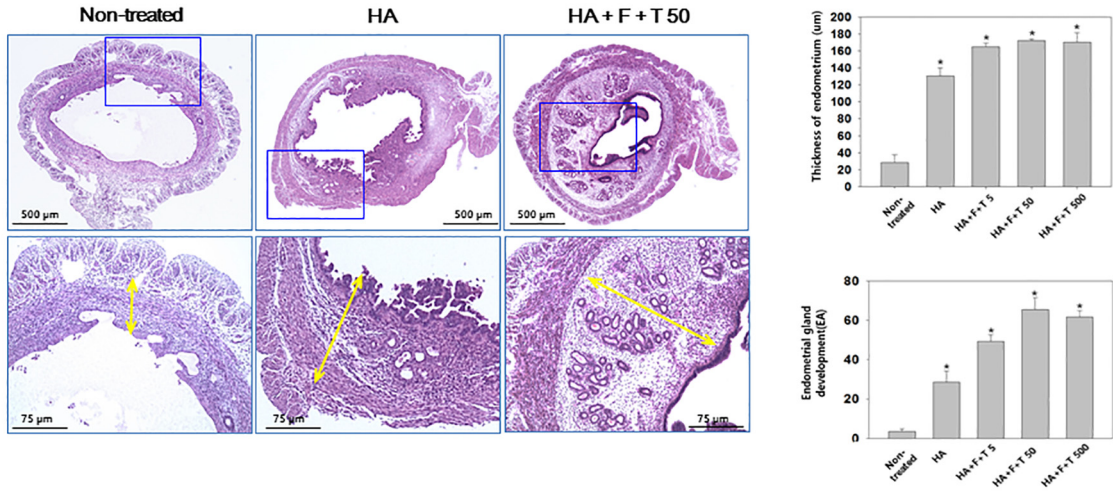
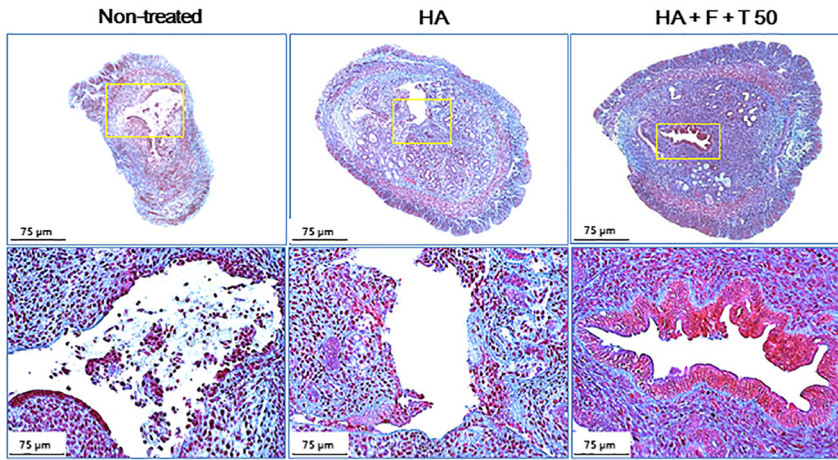


Fig. 2. Characterization of injectable HA hydrogel. Scanning electron microscopy and rheometry were performed to analyze the physical properties of the injectable HA hydrogels. Decidual features of the cells were maintained, even after mixing with hydrogel. A. Structural analysis of the HA/fibrin complex, constructed by the addition of different concentrations of thrombin, by scanning electron microscopy (SEM). B. Physical properties were analyzed by multiple rheometric measurements. F: fibrinogen, HA: hyaluronic acid, T: thrombin. C. Time course of dEMSC integration into HA/fibrin hydrogels analyzed by scanning electron microscopy and confirmation of encapsulation. D. Cross-sectional SEM images of dEMSCs embedded hydrogel for the evaluation of distribution and encapsulation of dEMSCs within hydrogel. E. Effective harboring of cells in HA/fibrin hydrogels was demonstrated by Desmin immunostaining. F. Survival of cells in HA/fibrin hydrogels (WST-1) was measured by absorbance. G-H. Expression of cell adhesion- and ECM-related genes (G) and of decidua-specific genes (H) was confirmed in HA/fibrin hydrogels encapsulating dEMSCs (qRT-PCR).

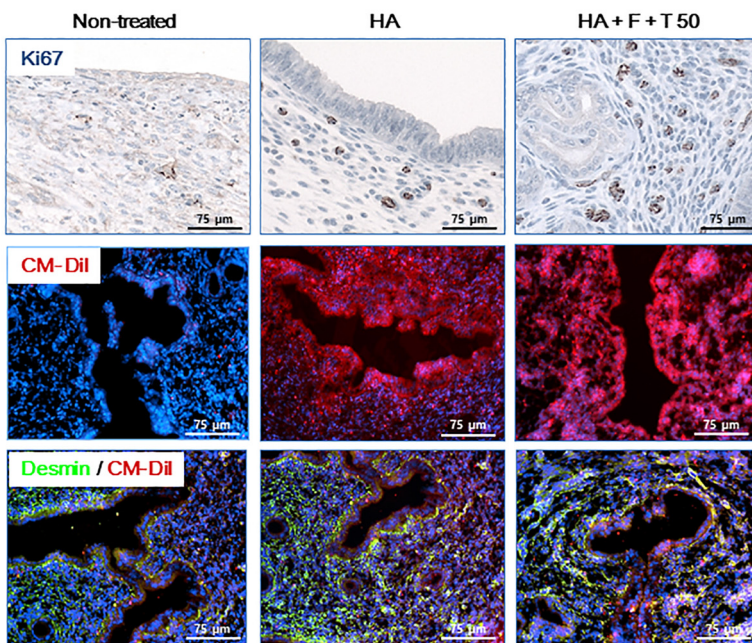
A



B



C



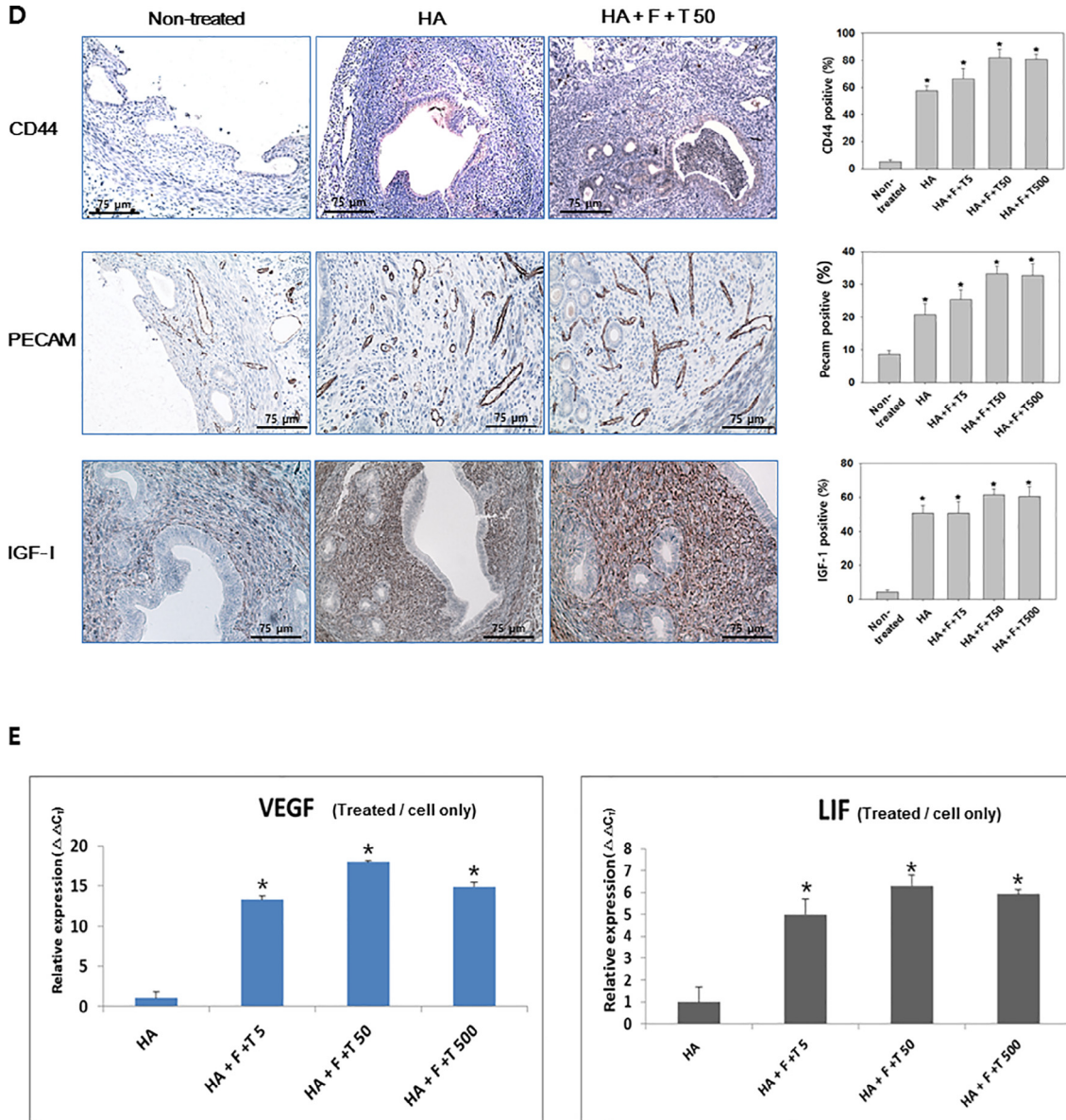


Fig. 3 (continued)

groups than in the HA-only group, with the H + F + T50 group showing the highest levels ($P < 0.01$, Fig. 3E).

Taken together, these results indicated that engraftment of HA/fibrin hydrogels regenerated damaged uteri by accelerating cell-cell adhesion between the remaining cell layer and the injected DEMSCs.

3.5. Functional recovery after HA/fibrin hydrogel treatment

3.5.1. Implantation of embryos onto the regenerated endometrium

Blastocyst-stage embryos (E3.0) were transferred to the regenerated endometrium, and their implantation was confirmed by staining with Evans blue, an azo dye with a very high affinity for

Fig. 3. Regeneration of endometrium in engrafted synechiae model. Regeneration of the endometrium in a murine model of endometrial damage was evaluated by measuring the increase in endometrial thickness and portion of fibrous tissue after treatment. The engraftment of injected cells was confirmed by co-expression of specific markers. The expression of endometrium-specific markers was evaluated at the mRNA level. A. Histological analyses of endometrial thickness and the number of glands in regenerated endometria. The HA + F + T50 group was most effective at inducing endometrial regeneration. B. Masson trichrome (MT) staining for the measurement of fibrous tissue (blue, indication of scar) in each group. The HA + F + T50 group demonstrated lower contents of fibrous tissue than non-treated and HA + F + T5 groups. C. Ki67-positivity indicated that cells were engrafted (brown) and had proliferative activity. Engrafted cells were pre-labeled with CM-Dil, and co-localization with Desmin indicated regeneration of the endometrium. D. Immunohistochemistry of neovascularization-related and decidual-specific markers, CD44, PECAM, and IGF-1. *F: fibrinogen, HA: hyaluronic acid, T: thrombin. E. Expression of VEGF and LIF in HA/fibrin hydrogels (qRT-PCR). *LIF: leukemia inhibitory factor, VEGF: vascular endothelial growth factor. (For interpretation of the references to colour in this figure legend, the reader is referred to the web version of this article.)

serum albumin. Examination of the uterine horns when embryos were at day 7.5 and day 10.5 showed that the implantation rate of the HA + F + T50 hydrogel group was significantly higher than the rate observed in the nontreated and HA-only groups (Fig. 4A). The implantation rate after donor embryo transfer in treated animals was higher in the HA/fibrin groups than in the HA-only group (Table 4).

Transverse sections of the uteri were prepared to evaluate postimplantation embryonic development. At 3 days after implantation, ectoplacental cone (epc) development was observed on the inner side of the uterine cavity (Fig. 4B, left panel). In addition, the expression of stage-specific embryonic antigen (SSEA)-1, an important factor in cell adhesion and migration, was evaluated. SSEA-1-positive cells were distributed over the entire transverse section (Fig. 4B, right panel).

3.5.2. Expression of three embryonic germ layer markers

The development of the three germ layers in implanted embryos was confirmed at E7.5 by measuring the expression of the specific markers *sox2* (ectoderm), Brachyury (mesoderm), and hepatocyte nuclear factor 4 alpha (HNF4 α , endoderm) and at E8.5 by measuring the expression of the specific markers Nestin (ectoderm), Brachyury, and alpha-fetoprotein (α FP, endoderm, Fig. 4C). Morphological analysis of developing embryos from the engrafted groups at E13.5 and of neonates showed normal development as compared to nondamaged controls (Fig. 4D).

Taken together, these results indicated that the embryos implanted on the regenerated endometrium developed normally,

with no significant differences compared to those of the nondamaged control group.

4. Discussion

The endometrium, the inner layer of the uterus, is the main location for embryo attachment, adhesion to the receptive epithelium, and trophoblast invasion [26]. Endometrial damage, caused by physical wounds or infection, leads to infertility due to nonattachment or miscarriage.

To the best of our knowledge, this is the first report confirming the therapeutic efficacy of injectable HA/fibrin hydrogels containing dEMSCs for the repair of uterine synechiae in a murine model. Our data showed significant regenerative effects of the *in vitro* processed isotopic cells encapsulated in composite scaffold materials. Attempt at pregnancy was possible as early as 2 weeks after treatment, and the successful *in vivo* embryonic implantation and development in the regenerated recipient model was confirmed at 7 days after ET.

Previous studies demonstrating similar therapeutic effects have several limitations. They used only heterotopic cells, such as BM-MSCs with [21] or without collagen [22], and human embryonic stem cell (hESC)-derived endometrium-like cells [23]. Furthermore, cell production required up to 5 weeks, and the time required before the first pregnancy attempt was as long as 90 days after treatment. Only one group used a commercially available collagen membrane, but its insertion was possible only

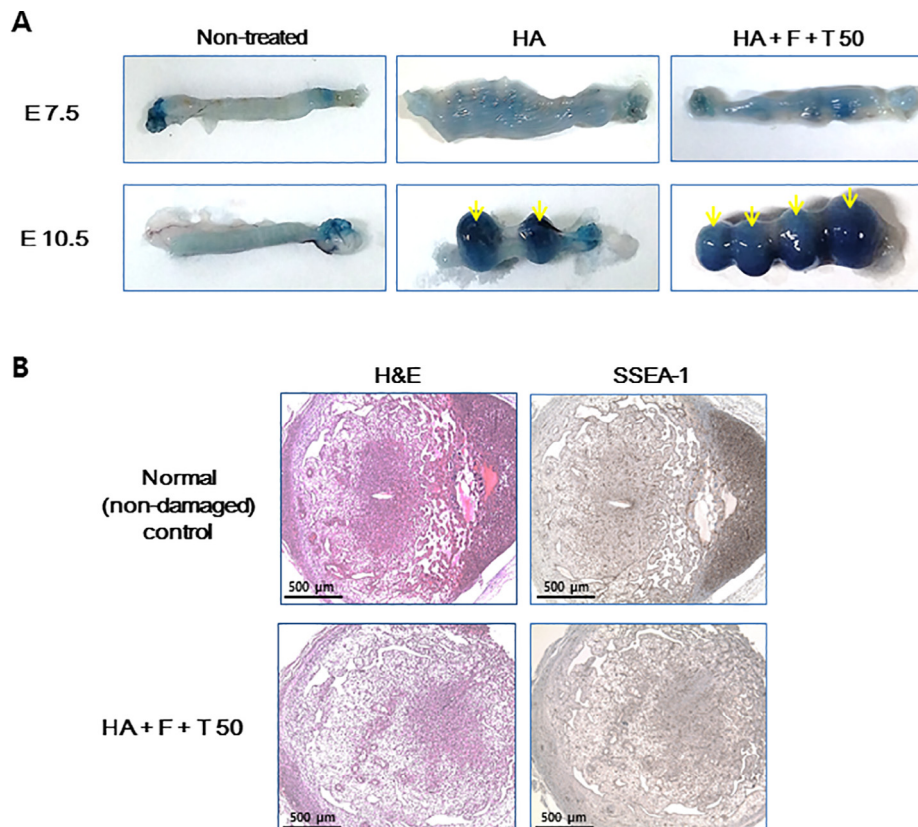


Fig. 4. Functionality of endometrium treated with injectable HA/fibrin hydrogels. The function of the regenerative endometrium was evaluated by analyzing the implantation of transferred embryos. Implantation and normal early gastrulation were confirmed, and the birth of offspring was also evaluated. A. Evans blue staining of uterine horns, at E7.5 and E10.5, showed that the HA/fibrin hydrogel group showed a significantly higher implantation rate than nontreated control and HA-only groups. B. Cross-section of uterus containing the implanted embryo. The formation of ectoplacental cone with embryo-specific SSEA-1 expression was observed. C. Expression of three germ layer markers, Sox2/Brachyury/HNF4 α , at E7.5 (upper panel) and Nestin/Brachyury/ α FP at E8.5 (lower panel), in developing embryos. D. E13.5 embryos and neonates from the hydrogel-treated group showed normal development comparable to that of nondamaged control animals. E: embryonic day, F: fibrinogen, HA: hyaluronic acid, H&E: hematoxylin and eosin, T: thrombin.

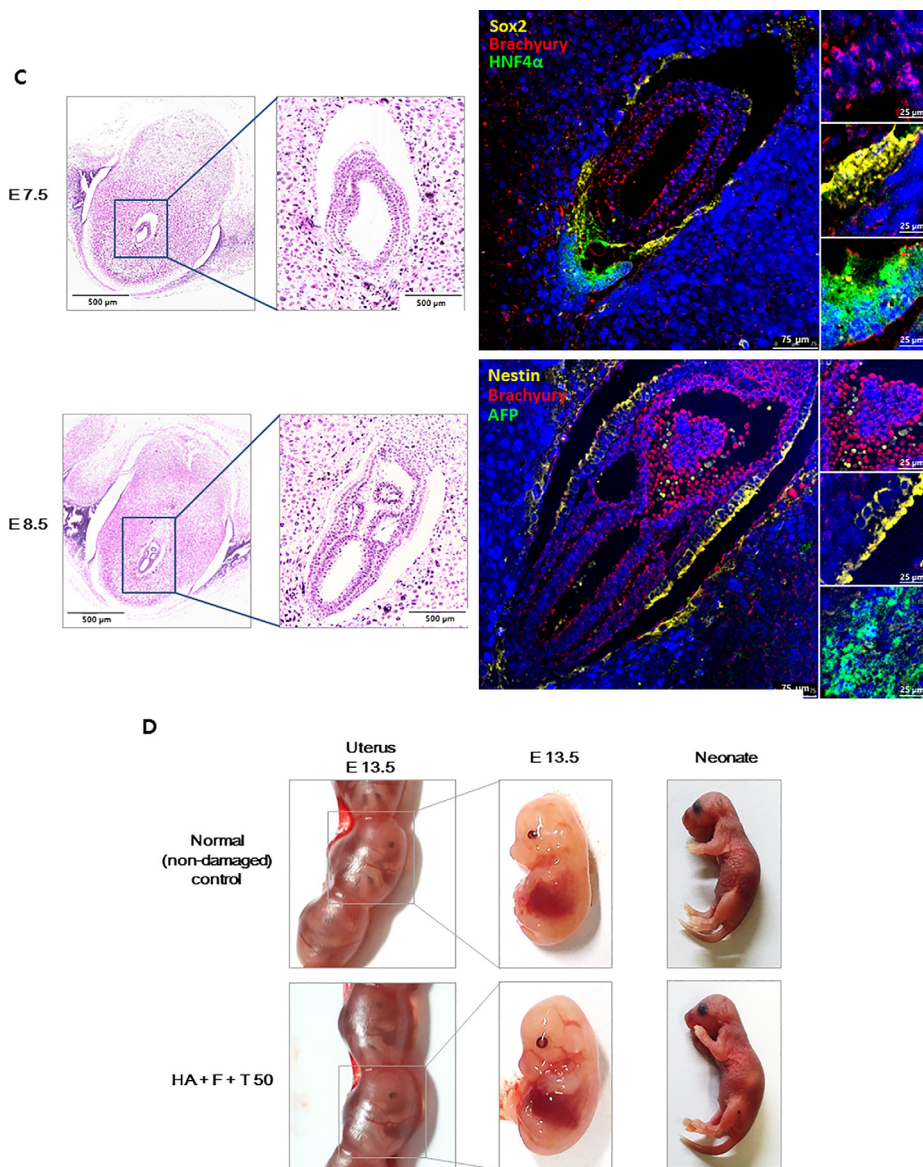


Fig. 4 (continued)

Table 4
Embryo implantation rate in hydrogel-treated murine synechia model.

Treatment	Number of animals	Number of transferred embryos (a)	Number of implanted embryos (b)	Percent of embryo implantation (b/a)
Nontreated	8	80	0	0%
HA	8	80	5	6.3%
HA + F + T 5	8	80	29	36.3%
HA + F + T 50	8	80	37	46.3%

HA: hyaluronic acid, F: fibrinogen, T: thrombin.

through invasive major abdominal and uterine surgical procedures.

Comparatively, in our study, bioprocessed isotopic cells were chosen for the treatment of damaged uteri, and efficient regenerative therapeutic effects, accompanied by shorter recovery times, were achieved. Endometrial cells were used after *in vitro* decidualization and were engrafted through a small dorsal incision [27], which is significantly less invasive and simpler than previously reported procedures.

The decidua comprises specialized endometrial cells, which prepare the uterus for embryonic implantation. It is well known that these cells control trophoblast invasion and protect the placental semi-allograft against maternal immune responses [28]. Assuming that the BM-MSCs and hESC-derived EMSC-like cells that were used in the previous studies were not sufficiently specialized, we sought to use cells that were physiologically compatible with the intrauterine environment, i.e., decidua or decidualized cells. However, the primary culture of decidual cells isolated from

pregnant animals is impractical, as optimal culture conditions have not yet been established. Therefore, using *in vitro* decidualized EMSCs was considered the most feasible option for generating therapeutic cell–biomaterial constructs.

The cells used in our study were selected based on immunophenotyping and the efficiency of the *in vitro* decidualization process. Cells from parous animals showed superior decidualization efficiency compared to cells from immature animals. The CD expression profile of these cells was maintained after *in vitro* decidualization. CD44 expression is related to integrin and plays an important role in the process of embryonic implantation. CD44 is also the major surface receptor for HA and is implicated in cell–matrix adhesion and cell migration progresses [29–31].

HA is a well-characterized biomaterial that has been previously used for cell delivery, and it can induce lineage-specific cell differentiation. However, despite many advantages, HA cannot mediate cell attachment owing to its low viscosity. Fibrin has independently been used as an injectable biomaterial in tissue engineering applications [32] owing to its capacity to support cell growth, migration, and proliferation and stem cell differentiation [33,34]. However, fibrin hydrogels have poor mechanical properties [35,36], and they are typically used in combination with other biomolecules such as HA because this leads to enhanced cell growth and engraftment [37].

In an effort to regenerate the endometrium, HA has been used in various damaged models [38–42]. A correlation has been established between the HA level and endometrial receptivity toward preimplanting embryos. This result parallels the high concentration of HA observed in the remodeling tissue [43]. In normal female physiology, HA is increasingly deposited during the embryonic implantation, which, however, declines afterwards [44]. Furthermore, HA-positive endometrium has been shown to be related to placental vascularization [45].

Among different hydrogels, HA with endometrial stromal cells seems to be the most suitable for the regeneration of endometrium, as HA interacts with ECMs and contributes to the matrix molecules. Previous studies [46] suggest that the HA receptors exist during every estrous cycle, while their contents may vary from cycle to cycle. HA is degraded by hyaluronidase, which is highly expressed in the peritoneum and endometrium [39].

In this study, we constructed HA/fibrin hydrogels using concentrations of T optimized to accelerate cross-linking and facilitate the delivery of efficiently conditioned cells. As this conditioning may affect treatment efficiency [47], we examined the effects of different T concentrations on stiffness to construct the most suitable HA/fibrin hydrogels. The degree of stiffness was sufficient, such that the cells could be integrated and easily engrafted onto the damaged surface of the endometrium.

The stiffness of other female reproductive organs such as the cervix and vagina is much higher owing to their thickness and solid structure. The stiffness of uterine tissues has often been assessed when examining uterine fibroids. However, uterine fibroid tissue possesses larger amounts of altered and disordered collagen, and thus, reducing the stiffness of uterine tissue is considered as an alternative therapeutic option for fibroid treatments [48]. By contrast, the endometrium is very thin and soft and is involved in the regular release of menstrual blood and the invasion of embryos. Our data provide insights into the requisite stiffness for the treatment of endometrial lesions. Mixing the cells with hydrogel prevents the loss of cells injected into the uterine horns. It is important that injected cells be retained within uterus for the engraftment of dEMSCs to damaged endometrium. Therefore, the limiting mobility of cross-linkage with porosity may be important for the regeneration of the endometrium.

This is among the first reports, to the best of our knowledge, describing the ideal stiffness of HA/fibrin hydrogels encapsulating

dEMSCs. The HA + F + T50 hydrogel was the most efficient of those tested in our study, suggesting that it held the cells more efficiently. Moreover, we have demonstrated the differences in physical stiffness and pore architecture of various HA/fibrin hydrogels, which are important properties affecting their ability to transport important molecules and other nutrients [49].

In our study, the embryo implantation rate in hydrogel-treated group was significant. We assumed that the production of LIF would increase after efficient endometrial regeneration. The importance of LIF during embryonic implantation has been reported in a previous study [50], and its expression in mice always precedes blastocyst implantation. It can be inferred from our results that LIF, secreted after hydrogel–cell treatment, played a supportive role in the observed therapeutic effects.

In this investigation, the therapeutic efficiency of the treatment was assessed by measuring embryonic implantation rate, i.e., the number of implantation sites divided by the number of embryos transferred. In contrast, previous reports utilized only natural mating; therefore, such quantitative implantation data were not reported. We transferred a defined number of embryos per animal, and our data showed that the embryonic implantation rate of injectable hydrogel-treated animals was comparable to the rate seen in the nondamaged control group (Table 4).

Cautious interpretation of our results is necessary on some points. First, our data showed that the most effective T concentration was 50 mIU/mL rather than 500 mIU/mL. A higher T concentration may have superior networking properties; however, gelation time and degree of viscosity should also be considered when deciding the most efficient concentration of T. Second, although we used the same strain of mice, i.e., isogenic rather than allogenic, the characteristic semi-allogenic immunogenicity of the maternal–fetal interaction should be taken into consideration. Third, when applying this treatment strategy to humans, the injectable hydrogels should be further optimized for a single uterus supporting a singleton pregnancy, which differs from murine double uteri supporting multiple pregnancies.

5. Conclusions

Our study confirmed the therapeutic efficacy of HA/fibrin hydrogels containing dEMSCs for the repair of significantly damaged endometria in a murine model. Engrafted cells were well integrated, and the expression of decidua-related, cell adhesion molecules was confirmed. Embryonic implantation data showed that the treatment modality of using injectable hydrogel is efficient for the regeneration of damaged endometrium. This innovative strategy of using *in vitro* processed isotopic cells encapsulated in injectable composite hydrogels can not only shorten recovery time but also achieve significant treatment outcomes.

Acknowledgements

This study was supported by grants from the Ministry of Science and ICT (2016R1E1A1A01943455 and 2016R1D1A1A02937287). The authors would like to express sincere thanks to Dr. Amin Tamadon, Seung Hun Park, Kyung Mee Cho, Bo Bin Choi, Kyusun Han, Eun Bee Shin, and Kyoungmin Noh for technical assistance.

Conflict of interest

The authors have declared that there are no conflicts of interest.

References

- [1] R. Deans, J. Abbott, Review of intrauterine adhesions, *J. Minim. Invasive Gynecol.* 17 (5) (2010) 555–569.

- [2] P. Gambadauro, J. Gudmundsson, R. Torrejon, Intrauterine adhesions following conservative treatment of uterine fibroids, *Obstet. Gynecol. Int.* 2012 (2012) 853269.
- [3] C.M. March, Asherman's syndrome, *Semin. Reprod. Med.* 29 (2) (2011) 83–94.
- [4] Y.J. Kim, Y.Y. Kim, J.H. Shin, H. Kim, S.Y. Ku, C.S. Suh, Variation in microRNA expression profile of uterine leiomyoma with endometrial cavity distortion and endometrial cavity non-distortion, *Int. J. Mol. Sci.* 19 (9) (2018).
- [5] Y.J. Kim, Y.Y. Kim, D.W. Kim, J.K. Joo, H. Kim, S.Y. Ku, Profile of microRNA expression in endometrial cell during in vitro culture according to progesterone concentration, *Tissue Eng. Regen. Med.* 14 (5) (2017) 617–629.
- [6] Y.J. Kim, Y.Y. Kim, D.Y. Song, S.H. Lee, C.W. Park, H. Kim, S.Y. Ku, Proliferation profile of uterine endometrial stromal cells during in vitro culture with gonadotropins: recombinant versus urinary follicle stimulating hormone, *Tissue Eng. Regen. Med.* (2018), <https://doi.org/10.1007/s13770-018-0156-4>.
- [7] S.Y. Ku, Y.M. Choi, C.S. Suh, S.H. Kim, J.G. Kim, S.Y. Moon, J.Y. Lee, Effect of gonadotropins on human endometrial stromal cell proliferation in vitro, *Arch. Gynecol. Obstet.* 266 (4) (2002) 223–228.
- [8] C.Y. Ramathal, I.C. Bagchi, R.N. Taylor, M.K. Bagchi, Endometrial decidualization: of mice and men, *Semin. Reprod. Med.* 28 (1) (2010) 17–26.
- [9] S.K. Dey, How we are born, *J. Clin. Invest.* 120 (4) (2010) 952–955.
- [10] I.A. Maslar, D.H. Riddick, Prolactin production by human endometrium during the normal menstrual cycle, *Am. J. Obstet. Gynecol.* 135 (6) (1979) 751–754.
- [11] L.C. Giudice, B.A. Dsupin, J.C. Irwin, Steroid and peptide regulation of insulin-like growth factor-binding proteins secreted by human endometrial stromal cells is dependent on stromal differentiation, *J. Clin. Endocrinol. Metab.* 75 (5) (1992) 1235–1241.
- [12] B. Tang, S. Guller, E. Gorpide, Mechanisms involved in the decidualization of human endometrial stromal cells, *Acta Eur. Fertil.* 24 (5) (1993) 221–223.
- [13] F. Behzad, M.W. Seif, S. Campbell, J.D. Aplin, Expression of two isoforms of CD44 in human endometrium, *Biol. Reprod.* 51 (4) (1994) 739–747.
- [14] H. Singh, J.D. Aplin, Adhesion molecules in endometrial epithelium: tissue integrity and embryo implantation, *J. Anat.* 215 (1) (2009) 3–13.
- [15] D.D. Allison, K.J. Grande-Allen, Review. Hyaluronan: a powerful tissue engineering tool, *Tissue Eng.* 12 (8) (2006) 2131–2140.
- [16] R. Zhu, Y.H. Huang, Y. Tao, S.C. Wang, C. Sun, H.L. Piao, X.Q. Wang, M.R. Du, D.J. Li, Hyaluronan up-regulates growth and invasion of trophoblasts in an autocrine manner via PI3K/AKT and MAPK/ERK1/2 pathways in early human pregnancy, *Placenta* 34 (9) (2013) 784–791.
- [17] A. Simon, A. Safran, A. Revel, E. Aizenman, B. Reubinoff, A. Porat-Katz, A. Lewin, N. Laufer, Hyaluronic acid can successfully replace albumin as the sole macromolecule in a human embryo transfer medium, *Fertil. Steril.* 79 (6) (2003) 1434–1438.
- [18] J. Zhao, Q. Zhang, Y. Wang, Y. Li, Uterine infusion with bone marrow mesenchymal stem cells improves endometrium thickness in a rat model of thin endometrium, *Reprod. Sci.* 22 (2) (2015) 181–188.
- [19] H. Du, H.S. Taylor, Contribution of bone marrow-derived stem cells to endometrium and endometriosis, *Stem Cells* 25 (8) (2007) 2082–2086.
- [20] M. Ulukus, Stem cells in endometrium and endometriosis, *Women's Health* 11 (5) (2015) 587–595.
- [21] L. Ding, X. Li, H. Sun, J. Su, N. Lin, B. Peault, T. Song, J. Yang, J. Dai, Y. Hu, Transplantation of bone marrow mesenchymal stem cells on collagen scaffolds for the functional regeneration of injured rat uterus, *Biomaterials* 35 (18) (2014) 4888–4900.
- [22] F. Alawadhi, H. Du, H. Cakmak, H.S. Taylor, Bone Marrow-Derived Stem Cell (BMDSC) transplantation improves fertility in a murine model of Asherman's syndrome, *PLoS One* 9 (5) (2014) e96662.
- [23] T. Song, X. Zhao, H. Sun, X. Li, N. Lin, L. Ding, J. Dai, Y. Hu, Regeneration of uterine horns in rats using collagen scaffolds loaded with human embryonic stem cell-derived endometrium-like cells, *Tissue Eng. Part A* 21 (1–2) (2015) 353–361.
- [24] H. Zhao, L. Ma, J. Zhou, Z. Mao, C. Gao, J. Shen, Fabrication and physical and biological properties of fibrin gel derived from human plasma, *Biomed. Mater.* 3 (1) (2008) 015001.
- [25] Q. Xu, H. Duan, L. Gan, X. Liu, F. Chen, X. Shen, Y.Q. Tang, S. Wang, MicroRNA-1291 promotes endometrial fibrosis by regulating the ArhGAP29-RhoA/ROCK1 signaling pathway in a murine model, *Mol. Med. Rep.* 16 (4) (2017) 4501–4510.
- [26] A.C. Enders, R.K. Enders, S. Schlafke, An electron microscope study of the gland cells of the mink endometrium, *J. Cell Biol.* 18 (1963) 405–418.
- [27] Y.Y. Kim, B.B. Choi, J.W. Lim, Y.J. Kim, S.Y. Kim, S.Y. Ku, Efficient production of murine uterine damage model, *Tissue Eng. Regen. Med.* (2018), <https://doi.org/10.1007/s13770-018-0149-3>.
- [28] B. Gellersen, I.A. Brosens, J.J. Brosens, Decidualization of the human endometrium: mechanisms, functions, and clinical perspectives, *Semin. Reprod. Med.* 25 (6) (2007) 445–453.
- [29] H. Zhu, N. Mitsuhashi, A. Klein, L.W. Barsky, K. Weinberg, M.L. Barr, A. Demetriou, G.D. Wu, The role of the hyaluronan receptor CD44 in mesenchymal stem cell migration in the extracellular matrix, *Stem Cells* 24 (4) (2006) 928–935.
- [30] Z. Yang, P. Dong, X. Fu, Q. Li, S. Ma, D. Wu, N. Kang, X. Liu, L. Yan, R. Xiao, CD49f acts as an inflammation sensor to regulate differentiation, adhesion, and migration of human mesenchymal stem cells, *Stem Cells* 33 (9) (2015) 2798–2810.
- [31] J. Dzwonek, G.M. Wilczynski, CD44: molecular interactions, signaling and functions in the nervous system, *Front. Cell. Neurosci.* 9 (2015) 175.
- [32] S. Illien-Junger, G. Pattappa, M. Peroglio, L.M. Benneker, M.J. Stoddart, D. Sakai, J. Mochida, S. Grad, M. Alini, Homing of mesenchymal stem cells in induced degenerative intervertebral discs in a whole organ culture system, *Spine* 37 (22) (2012) 1865–1873.
- [33] T.A. Ahmed, E.V. Dare, M. Hincke, Fibrin: a versatile scaffold for tissue engineering applications, *Tissue Eng. Part B* 14 (2) (2008) 199–215.
- [34] P.A. Janmey, J.P. Winer, J.W. Weisel, Fibrin gels and their clinical and bioengineering applications, *J. R. Soc. Interface* 6 (30) (2009) 1–10.
- [35] Z.H. Syedain, J. Bjork, L. Sando, R.T. Tranquillo, Controlled compaction with ruthenium-catalyzed photochemical cross-linking of fibrin-based engineered connective tissue, *Biomaterials* 30 (35) (2009) 6695–6701.
- [36] S.L. Rowe, J.P. Stegemann, Microstructure and mechanics of collagen-fibrin matrices polymerized using anodized snake venom enzyme, *J. Biomech. Eng.* 131 (6) (2009) 061012.
- [37] J. Meinhart, M. Fussenegger, W. Hobling, Stabilization of fibrin-chondrocyte constructs for cartilage reconstruction, *Ann. Plastic Surg.* 42 (6) (1999) 673–678.
- [38] I.M. El-Sherbiny, M.H. Yacoub, Hydrogel scaffolds for tissue engineering: progress and challenges, *Glob. Cardiol. Sci. Pract.* 2013 (3) (2013) 316–342.
- [39] K. Nomura, K. Murakami, M. Shozu, T. Nakama, N. Yui, M. Inoue, Local application of danazol-loaded hyaluronic acid hydrogel to endometriosis in a rat model, *Fertil. Steril.* 85 (Suppl 1) (2006) 1157–1167.
- [40] V.H. Perez-Luna, O. Gonzalez-Reynoso, Encapsulation of biological agents in hydrogels for therapeutic applications, *Gels* 4 (3) (2018).
- [41] H.L. Xu, J. Xu, B.X. Shen, S.S. Zhang, B.H. Jin, Q.Y. Zhu, D.L. ZhuGe, X.Q. Wu, J. Xiao, Y.Z. Zhao, Dual regulations of thermosensitive heparin-polyoxamer hydrogel using epsilon-polylysine: bioadhesivity and controlled KGF release for enhancing wound healing of endometrial injury, *ACS Appl. Mater. Interfaces* 9 (35) (2017) 29580–29594.
- [42] A. Tamadon, K.H. Park, Y.Y. Kim, B.C. Kang, S.Y. Ku, Efficient biomaterials for tissue engineering of female reproductive organs, *Tissue Eng. Regen. Med.* 13 (5) (2016) 447–454.
- [43] A.M. Affy, S. Craig, A.F. Paulino, Temporal variation in the distribution of hyaluronic acid, CD44s, and CD44v6 in the human endometrium across the menstrual cycle, *Appl. Immunohistochem. Mol. Morphol.* 14 (3) (2006) 328–333.
- [44] L.A. Salamonsen, S. Shuster, R. Stern, Distribution of hyaluronan in human endometrium across the menstrual cycle. Implications for implantation and menstruation, *Cell Tissue Res.* 306 (2) (2001) 335–340.
- [45] J.J. Brown, V.E. Papaioannou, Distribution of hyaluronan in the mouse endometrium during the periimplantation period of pregnancy, *Differentiation* 52 (1) (1992) 61–68.
- [46] J.A. Gomes, R. Amankwah, A. Powell-Richards, H.S. Dua, Sodium hyaluronate (hyaluronic acid) promotes migration of human corneal epithelial cells in vitro, *Br. J. Ophthalmol.* 88 (6) (2004) 821–825.
- [47] M.D. Vardy, T.R. Gardner, F. Cosman, R.J. Scotti, M.S. Mikhail, A.O. Preiss-Bloom, J.K. Williams, J.M. Cline, R. Lindsay, The effects of hormone replacement on the biomechanical properties of the uterosacral and round ligaments in the monkey model, *Am. J. Obstet. Gynecol.* 192 (5) (2005) 1741–1751.
- [48] F.L. Jayes, B. Liu, F.T. Moutos, M. Kuchibhatla, F. Guilak, P.C. Leppert, Loss of stiffness in collagen-rich uterine fibroids after digestion with purified collagenase *Clostridium histolyticum*, *Am. J. Obstet. Gynecol.* 215 (5) (2016). 596 e1–596 e8.
- [49] A.K. Yu, T.W. Shek, Hydroxyapatite formation on implanted hydrogel intraocular lenses, *Arch. Ophthalmol.* 119 (4) (2001) 611–614.
- [50] C.L. Stewart, The role of leukemia inhibitory factor (LIF) and other cytokines in regulating implantation in mammals, *Ann. N. Y. Acad. Sci.* 734 (1994) 157–165.